Single channel surface electromyogram deconvolution to explore motor unit discharges

Medical & Biological Engineering & Computing manuscript No.
(will be inserted by the editor)

Single channel surface electromyogram deconvolution to explore motor unit discharges

Luca Mesin

Received: date / Accepted: date

Abstract Interference surface electromyogram (EMG) reflects many bioelectric properties of active motor units (MU), which are however difficult to estimate due to the asynchronous summation of their discharges. This paper introduces a deconvolution technique to estimate the cumulative firings of MUs. Tests in simulations show that the power spectral density of the estimated MU firings has a low frequency peak corresponding to the mean firing rate of MUs in the detection volume of the recording system, weighted by the amplitudes of MU action potentials. The peak increases in amplitude and its centroid shifts to higher frequency when MU synchronization is simulated (mainly due to the shift of discharges of large MUs). The peak is found even at high force levels, when such a contribution does not emerge from the EMG. This result is also confirmed in preliminary applications to experimental data. Moreover, the simulated cumulative firings of MUs are estimated with a correlation above 90% (considering frequency contributions up to 150 Hz), for all force levels.
The method requires a single EMG channel, thus being feasible even in applied studies using simple recording systems. It may open many potential applications, e.g., in the study of the modulation of MU firing rate induced by either fatigue or pathology and in coherency analysis.

Keywords Motor unit firing rate · motor unit synchronization · surface EMG · iterative reweighted least squares · L_1 optimization

L. Mesin
Mathematical Biology and Physiology, Department of Electronics and Telecommunications, Politecnico di Torino, Corso Duca degli Abruzzi 24, Torino, 10129 ITALY
Tel.: +39-0110904085
Fax: +39-0110904099
E-mail: luca.mesin@polito.it

1 Introduction

Contraction of muscle fibres is induced by bioelectric commands (i.e., action potentials propagating along their membrane) which could be non-invasively investigated by surface electromyogram (EMG). Many applications of EMG have been documented in the study of the control of motor units (MU), which was found to be affected by exerted force levels [2], fatigue [7], training [18] and pathology [20]. Moreover, decoding the MU recruitment strategy allows to investigate possible muscle synergies [12], common drive [11], coherence among different muscles [1] or the brain and a muscle [9].

The study of MU firings from surface EMG has relied mainly on two approaches.

1. Investigation of the power spectral density (PSD). The low frequency portion of the PSD until about 40 Hz of the raw signal [32], possibly after rectification [28], may show a peak reflecting MU firing statistics. However, the peak is not always visible from the raw data [32] and rectification (being non-linear) may impair the identification of neural strategies [30].
2. Decomposition of surface EMG [13][19] into trains of single MU action potentials (MUAP). This approach is computationally intensive, only a portion of the EMG energy can be recovered, processing EMG at high force levels is difficult [16], even if recent results suggest that decomposition can be successful up to force levels of 70% MVC, if many electrodes are used [17] (which is required to distinguish different MUAP shapes).

Thus, the first approach is simple, but not generally applicable; the second one is sophisticated, but it requires advanced recording systems and computationally intensive processing. A recent work proposed a fast and stable technique to split interference monopolar surface EMG from muscles with fibres parallel to the skin surface into propagating and non-propagating contributions [26]. The low frequency portion of the PSD of the non-propagating component was found to reflect the average MU discharge rate [27]. Reliable results could be obtained even with few electrodes (e.g., 3-4 electrodes) in monopolar configuration. However, many recording setups used in applications are based on a single acquisition channel, usually in single differential (SD) configuration, so that the above method cannot be applied.

This paper proposes a method to extract information on average MU firing rates from a single SD channel. It is based on a deconvolution procedure, which allows to approximate the recorded signal as the convolution of a prototype function (adapted to the signal) with an estimated firing pattern. The deconvolution problem is regularized (to enhance stability) and defined as a least L_1 error problem, obtaining a sparse solution [4], which resembles the cumulative firings of MUs.
The aim of this work is to describe this innovative method and to assess its ability to extract information on MU firing rates. Tests in simulations and preliminary applications on experimental data are discussed.

2 Methods

2.1 EMG deconvolution

The SD interference EMG was interpreted as the asynchronous summation of different MU contributions, assumed approximately equal to a single prototype function called kernel, possibly rescaled in amplitude. The kernel was defined as the first derivative of a Gaussian function, with standard deviation chosen optimally to fit the PSD of the original signal. Thus, the SD EMG was written as the convolution of the kernel with the firing pattern, to be estimated, which could be considered as a cumulative sum of MU discharges weighted by MUAP amplitudes (related to MU dimensions and locations).

Due to modelling approximations and to the presence of experimental noise, the EMG was assumed to be represented by the sum of the above-mentioned convolution and a perturbation

$$s(t) = K(t) * f(t) + n(t) \tag{1}$$

where $s(t)$ is the EMG, $K(t)$ is the kernel, $f(t)$ is the firing pattern and $n(t)$ is the perturbation (which is a function including all errors in approximating the data as the convolution of the kernel with the firing pattern, e.g., due to noise, differences between average MUAP shape and the kernel, heterogeneity of shapes of different MUAPs). Estimating the firing pattern is an unstable inverse problem, which should be regularized, e.g., considering the following Tykonov regularization approach [5]

$$argmin_{\hat{f}(t)} \left\| s(t) - K(t) * \hat{f}(t) \right\|_2^2 + \alpha \left\| \hat{f}(t) \right\|_2^2 \tag{2}$$

with α to be chosen considering the trade-off between a better fit of the data and stability of the solution. The problem was discretized as in [22], converting the convolution operator into a multiplication with the matrix A, including delayed versions of the kernel in its columns (i.e., the kernel is discretized with a sampling interval equal to the reciprocal of the sampling frequency and delayed of multiples of such an interval). The parameter α was selected equal to 1% of the maximum eigenvalue of $A^T A$. Notice that the number of elements of A increases as the square of the number of samples of the processed epoch. Thus, to reduce the computational cost, the signal epoch was split into small portions (of 125 ms, with about 31 ms of overlap) which were processed separately and then recombined.

The mean square error in (2) is convenient as it allows to get an analytical solution of the problem [5]. However, due to the square function (which emphasizes large values and reduces lower ones), the solution is sensitive to outliers and too tolerant to small values. Using the L_1 norm instead of the L_2, errors are weighted with respect of their amplitude instead of energy, resulting in a solution that is more stable to outliers and sparse (as small values, if useless, are put to zero). Sparse solutions are finding growing applications, e.g., in the field of compressed sensing [10]. However, solving a least L_1 problem

is difficult, as there is not an analytical solution, instead available for problem (2). The iterative reweighted least square (IRLS) method converts the L_1 problem into a weighted L_2 one for which the analytical solution can be found [5]. The weights are searched iteratively in order that the weighted L_2 problem approximates the original L_1 problem. IRLS was used here to minimize the L_1 error (same expression as in (2), but using average rectified values instead of mean squares), considering 10 iterations. Before each iteration, the solution was put to zero where it was negative (as the firing pattern should be non-negative; notice that this imposes a fixed polarity of MUAPs, which is reasonable only if the SD channel is placed between the innervation zone and a tendon in order to see unidirectional propagation of MUAPs; moreover, imposing the firing pattern to be positive, avoids unstable oscillations, leading to phase cancellations in the estimated data).

2.2 Test data

The same simulation model considered in [27] was used. In brief, single fibre action potentials (SFAP) were simulated using a cylindrical volume conductor (fat layer thickness of either 3 or 7 mm, symmetrical fibres with average semi-length of 60 mm, spread of innervation zone and tendons equal to 10 mm, sample frequency 2048 Hz), from which MUAPs were built. An SD channel was considered (with 10 mm of inter-electrode distance, IED; first electrode 15 mm distant from the centre of the innervation region).

The total number of simulated MUs was 400. Their conduction velocities (CV) were randomly chosen with Gaussian distribution with standard deviation 0.3 m/s and mean value in the range 3-5 m/s (0.5 m/s step).

The MU recruitment was simulated as in [8] mostly considering a high force level, i.e., 80% of the maximal voluntary contraction (MVC, except for a few preliminary examples and a final test with force level ranging between 2% and 100% MVC). This is a worst case condition for the algorithm, as the simulated MUs are all active and their discharges are very heterogeneous. It is also a condition in which the methods available in the literature cannot find a low frequency peak reflecting MU discharges. The firing rate (FR) distribution was changed in different simulations. Specifically, the FR distribution provided by the simulator was linearly changed to remap it in $[FR_{min}, FR_{max}]$, where FR_{max} was chosen in the range 20-40 Hz (with step 5 Hz) and $FR_{min} = 5$ Hz $+ 0.25\ FR_{max}$.

The coefficient of variation (COV) of the inter-spike interval (ISI) was either 10 or 20% in different simulations. The obtained MU discharges were either kept random or synchronized, obtaining an additional dataset. MU synchronization was simulated as in [25] (percentage of firings synchronized in each MU train and for each synchronization event assumed to be equal; this percentage was used to indicate the synchronization level). Interference EMGs of duration 10 s were simulated.

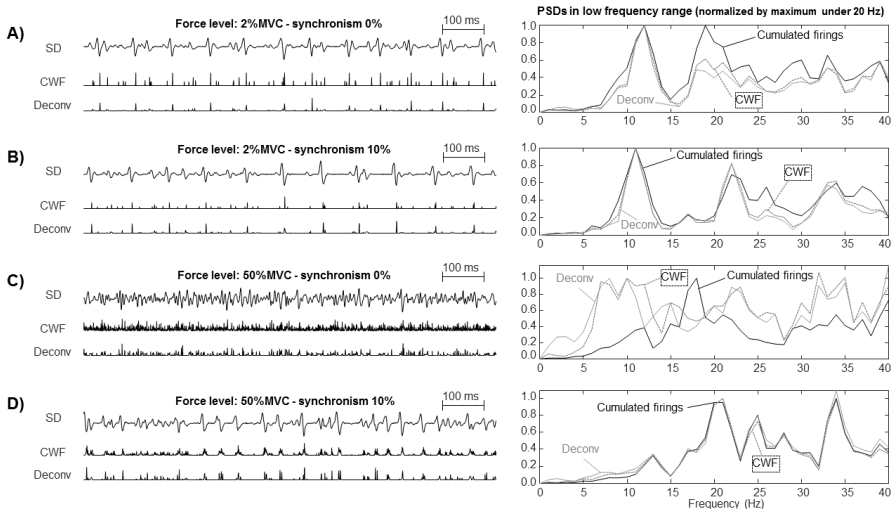

Fig. 1 Examples of simulated EMG, cumulative weighted firings (CWF) and estimated firings by deconvolution (Deconv), considering different levels of force (2% and 50% of maximal voluntary contraction, MVC, in A-B and C-D, respectively) and synchronization (either random firings or 10% of synchronization, in A-C and B-D, respectively). Portions of data are shown on the left, the power spectral densities (PSD) on the right (Welch method applied to 3 s of data, sub-epochs of 0.5 s, mean value removed from each of them, 50% of overlap).

The same experimental data were considered as in [27]: EMG from thenar muscle with a contraction level of 6% MVC (30 s duration) taken from the dataset of a previous study [31]; vastus lateralis and medialis at 20 and 40% MVC, respectively (10 s duration), chosen from the dataset of [14]. All recordings were acquired in isometric and isotonic conditions. The firing trains of some MUs were identified from these interference EMGs using a validated algorithm [19] applied on multi-channel data (from which a single SD was considered).

2.3 Assessment of performance

The PSDs of either simulated or estimated firings were computed by the Welch method (sub-epochs of 0.5 s, mean value removed from each of them, overlap of 50% and zero padding to get 1 Hz resolution).

The PSD of the estimated firings was compared to that of the cumulative firings of MUs (defined as the sum of their firing patterns) and of the cumulative weighted firings (CWF). The latter was defined as the sum of MU firing patterns weighted by the root mean square amplitude of the corresponding MUAP. This allows to account for the detection volume of the recording system.

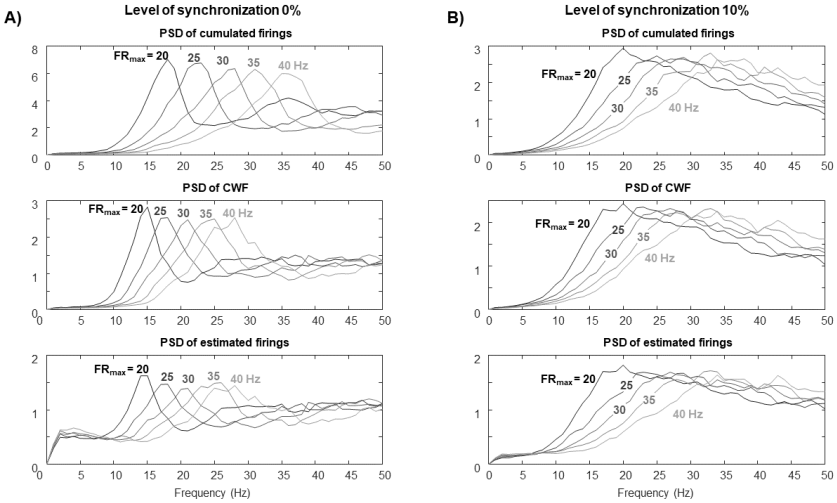

Fig. 2 Mean PSDs of cumulative firings, CWF and estimated firings obtained by averaging across 20 cases (corresponding to 2 thicknesses of the fat layer, 5 values of mean CV and 2 COVs of ISI), each with constant FR distribution of MUs. A) Not synchronized firings and B) 10% of synchronization.

3 Results

Some preliminary data are shown in Figure 1. For very low force levels (1A and 1B), the low frequency peak found in the PSD of the cumulative firings is the same as the one obtained considering either CWF or the firing pattern estimated by deconvolution. Indeed, few MUs are active and they are firing at a similar low rate. Considering a greater force level with random discharges (1C), the PSD of cumulative firings show a peak corresponding to the high frequency rate of the many small active MUs. On the other hand, the estimated firing pattern and the CWF provide similar information, biased by the largest MUs, which are firing at low rate. When firings are partially synchronized (1D), the three time series (cumulative firings, CWF and estimated firings) provide similar information, with a low frequency peak centred at a higher frequency than when discharges were not synchronized.

As original EMGs (either monopolar or SD, either rectified or not) do not show a low frequency peak for force levels higher than about 40% MVC [21][27], a high force level (80% MVC) was considered in the following tests in simulations. FR modulation was included to explore the possibility of investigating it by the low frequency peak of the firings estimated by deconvolution.

Figure 2 shows the mean PSDs of CWF and estimated firings obtained by averaging conditions with same maximal FR. Both the case of random (2A) and synchronized firings (2B) are considered. In the first case, the PSD of cumulative firings shows a low frequency peak close to the maximal FR, which is reached by many small MUs. The estimated firings show peaks with location and spread that resemble those of the CWF, representing FRs dis-

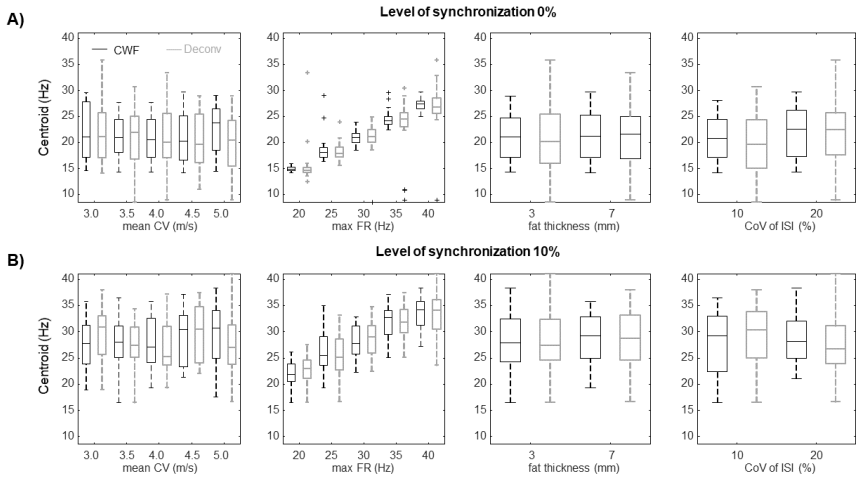

Fig. 3 Location of the low frequency peak of the PSD of the cumulative weighted firings (CWF) and of the firings obtained by deconvolution (Deconv). The parameter is given in terms of distributions (median, quartiles and range, with outliers shown individually) of values obtained by splitting with respect to different means of MU CV distributions, maximal FR, fat layer thickness and coefficient of variation (COV) of inter-spike interval (ISI). A) Random activation of MUs and B) 10% of synchronization of MU spikes.

tributions biased by large MUs in the detection volume of the SD channel. When firings are synchronized, the three firing patterns (cumulative firings, CWF and estimated firings) provide very similar information. Notice that the peaks are shifted toward higher frequency with respect to the case of random MU discharges.

Figure 3 shows the centroid of the low frequency peaks of the PSDs of CWF and estimated firings (computed as detailed in [27]). The centroids of the estimated firings reliably represent those obtained considering the CWF. They are affected by different FRs, but not by different mean CV, fat layer thickness and CoV of ISI (statistically significant effects indicated by 4-way ANOVA, with $p<0.001$). The centroid is affected by MU synchronization, i.e., its value is increased (paired Wilcoxon signed rank test, with $p<0.001$), as also noted in the previous figures.

Figure 4 shows the cross-correlation of the low frequency peaks found in the PSDs of the CWF and of the estimated firings. The frequency range in which the peak was considered was defined from 0 to the centroid plus 3 times the standard deviation of the peak identified below 50 Hz. High correlations were found in all conditions. In the case of random firings (4A), different CV, FR distributions and fat layer thickness induced no relevant effect, but lower correlation was found in case of greater CoV of ISI (statistically significant effect indicated by 4-way ANOVA, with $p<0.001$). Higher correlation (paired Wilcoxon signed rank test, with $p<0.001$) was obtained in the case of MU

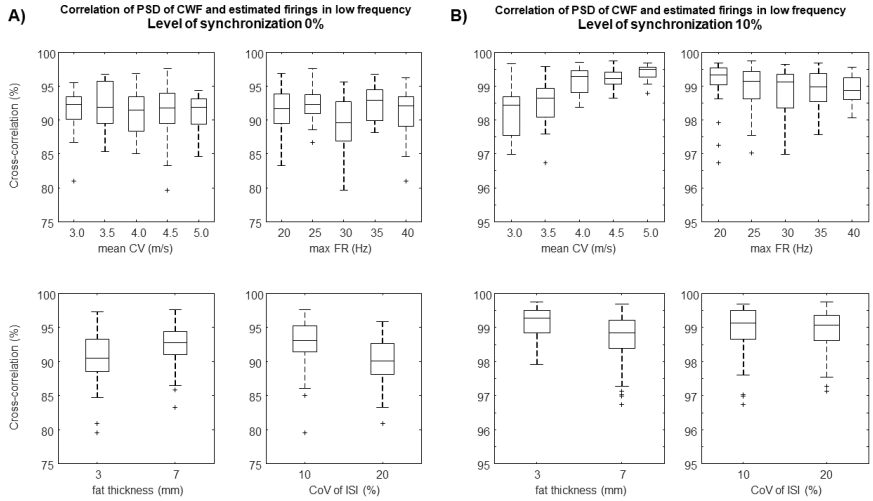

Fig. 4 Distributions of correlation coefficients of the PSD in the low frequency range of cumulative weighted firings (CWF) and firings estimated by deconvolution. The correlation coefficients are split with respect to different mean CV of MUs, maximal FRs, thickness of the fat layer and coefficient of variation (COV) of inter-spike interval (ISI). A) Random activation of MUs; B) 10% of synchronization of MU spikes.

synchronization, shown in 4B. Statistically significant effects of CV and fat layer thickness were disclosed by 4-way ANOVA, in this case.

Figure 5 shows examples of application to experimental data. With a small contraction level (thenar muscle, 5A), a low frequency peak is found also in the PSD of raw EMG (5D), but no peak is clearly visible for larger force levels (vastus lateratis and medialis, in 5E-F, respectively). On the other hand, a low frequency peak is always found in the PSD of the estimated firings (5G-I), which is consistent with that of the CWF, computed based on EMG decomposition by the method described in [19]. Notice some mismatch of the two peaks in the case of vastus lateralis: however, decomposition accounted only for a small portion of the total energy of the signal in such a case.

4 Discussion

Theoretical interpretations indicate that the PSD of EMG includes two main contributions [2]: the low frequency portion, affected by MU firing statistics, and the medium-high portion, reflecting the mean shape of MUAPs. Thus, the firing statistics could be approximately recovered by a deconvolution operation applied to the EMG, using a kernel reflecting the average MUAP shape. Here, the kernel was indeed fit to the PSD of the signal, in order to compensate for the MUAP shape and allow to better extract information on MU firing statistics. Deconvolution was computed after introducing a regularization term. Moreover, the IRLS method was used to approximate the L_1 fit of

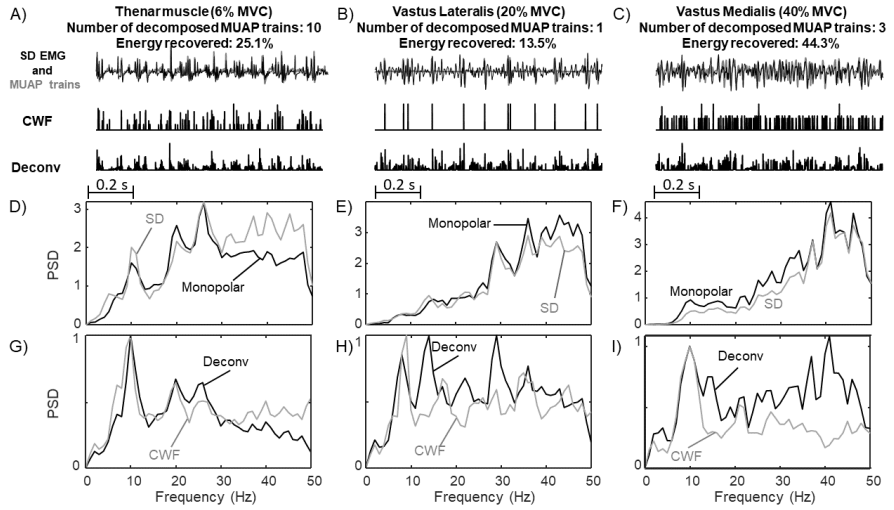

Fig. 5 Tests on experimental data: A) thenar muscle, B) vastus lateralis and C) vastus medialis (30 s, 10 s and 10 s of stationary contractions, respectively). EMG was decomposed by the method discussed in [19]. PSDs of monopolar and SD data in the low frequency range are shown normalized with respect to their energy in D), E) and F), for thenar, vastus lateralis and medialis muscles, respectively. The corresponding PSDs of the CWF and estimated firings (Deconv) are shown in G), H) and I) (normalization with respect to the maximum value). An equivalent figure is shown in [27], considering non-propagating components to estimate the low frequency peak.

the data. A fine tuning based on few preliminary tests was considered to select the penalty term α and the number of iterations of the IRLS method. An extensive search for the best parameters was not adopted, as both parameters have a main effect on the high frequency contribution of the estimated average MU discharges: indeed, reducing the penalty term, high frequency oscillations emerge and increasing the number of iterations of the IRLS method makes the solution sparser and more spiky (as the L_1 norm is better approximated). Thus, as noticed in preliminary tests, small effects are found in the low frequency range, if reasonable values of the two parameters are considered (e.g., penalization chosen in order to get a condition number of the matrix A^TA in the range 100-1000; number of iterations of the IRLS method between 5-20).

Power line interference, high frequency noise and baseline fluctuations (e.g., induced by movements artifacts) could reduce the quality of the signal. However, they could be reduced by preliminary processing (e.g., a notch filter to remove power line interference, low-pass and high-pass filters to attenuate high and low frequency interference, respectively). Moreover, the interpretation model used to represent the EMG is very simple. Indeed, MUAP shapes change across different MUs, e.g., due to their different locations and CVs. Thus, assuming that a single kernel could be used to represent all MUAPs is not correct and is expected to reflect into a reduced selectivity in identifying the discharge times. However, the tests indicate that the estimated firing

patterns have low frequency contributions that fairly represent the simulated discharges of MUs in the detection volume of the recorded channel. Specifically, information is retrieved on a weighted average of firing rates, with importance given to a MU firing pattern in relation to the amplitude of the corresponding MUAP. This could be considered as a limitation of the method, which is not able to provide information on the overall activity of the MUs of the target muscle, but is biased by MUAP amplitudes. However, consider that a bias induced by MUAP amplitudes (or even by their energies) affects the estimation of any EMG index (e.g., root mean square amplitude, CV or mean frequency). It is a problem of representativeness of surface EMG, which is more important as more selective spatial filters are used (e.g., double instead of single differential, or using smaller electrodes and IED), as they have a smaller detection volume.

MU synchronization has an important effect on the firing pattern. An increase of the low frequency contribution has been already predicted [33]. As the low frequency peak is more evident if discharges are synchronized, it is simpler to identify it in such a case (as shown in Figure 4). In addition, here the location of the low frequency peak was observed to shift toward higher frequency (Figures 1-3). This result can be interpreted considering that the largest MUs (which provide great contribution to the recorded EMG), after synchronizing to small MUs (which are firing at higher rates), may present some repeated discharges with high frequency. Figure 6 shows this result considering a simple simulation. Two only MUs are considered: a small MU firing at high rate (30 Hz) and a large one firing at low rate (about 22 Hz). Two conditions are considered, assuming either random or synchronized firings. In the first case, the phases of the firing pattern were random, but the ISI was constant (up to time resolution). The PSD of the cumulative firings (either the CWF or the one estimated by deconvolution) clearly shows the frequencies of the two MUAP trains (together with their harmonics), with larger weight given to the big MU, firing at lower rate (6A, bottom panel). Then, the firings have been synchronized with a level of 100% (so that all discharges of the great MU were synchronized with some firings of the small one). The firing patterns and the instantaneous firing rates show that there are bursts of few firings of the large MU at 30 Hz, separated by a silent period of irregular duration. Therefore, the PSD of the cumulative firings (6B, bottom panel) shows a clear peak at 30 Hz. The example is a hyper-simplification of MU activation (only 2 MUs are considered, which are firing either extremely regularly or perfectly synchronized), but it shows clearly the phenomenon underlying the drift of the low frequency peak of the CWF toward higher frequency induced by synchronization and observed in the simulations considered in Figures 1-3.

In experiments, discriminating the role of FR modulation and synchronization is an important and difficult task [25]. Tests on simulations indicate that the skewness of the distribution of the estimated firings provides some information on the level of synchronization: specifically, it increases with synchronization (as firings are more grouped). This observation could be deepened in the future, with the aim of investigating separately FR modulation and MU

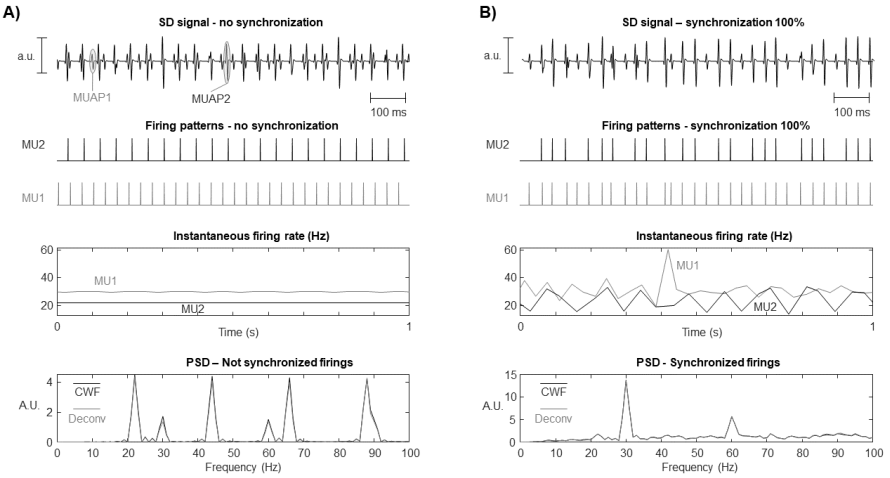

Fig. 6 Effect of MU synchronization in a synthetic case. A) Two MUs are considered, firing regularly at either 30 or 22 Hz, with no synchronization. A portion of SD signal (IED of 10 mm), the firing patterns, the instantaneous firing rate (defined as the reciprocal of the ISI computed for each pair of consecutive discharges) and the PSD are shown. B) Same as A), but after synchronizing the firings, with a level of 100% (i.e., all firings of MU 2 are synchronized with some of the firings of MU 1).

synchronization, which are two adjustments in MU behavior reflecting central responses to different stimulations, e.g., induced by training, fatigue or pathology.

Preliminary tests on experiments (Figure 5) show that the cumulative firings estimated by deconvolution always present a low frequency contribution, reflecting the average FR of MUs identified by a decomposition algorithm [19], even at high force levels, when the PSD of the raw data did not show any low frequency peak. This promising result will be further investigated in the future, considering a larger dataset of experimental data.

As the proposed method requires a single SD recording, there is the potential for applying it in many conditions in which high-density EMG is not available. Future applications could be foreseen in the study of FR modulation in different conditions, e.g., force levels [2], fatigue [7], training [18] and pathology [20]. Further investigation should also be devoted to the estimated firings in the time (instead of frequency) domain. The high temporal selectivity of the L_1 solution (providing sparse firings) could be useful to decode control strategies ruling muscle synergies [12], common drive [11] or coherence [3][9]. Moreover, recent outcomes indicate a strong association between MU discharges (extracted from high-density recordings) and kinematics, with potential use in the control of prostheses [6]. Thus, the firing pattern estimated by deconvolution could possibly provide an important feature to better control a myoelectric prosthesis, even using a single SD channel over each muscle of interest.

An important issue in prosthetics and related applications is processing data in real time. This requires to reduce the computational cost of the algorithm, as its processing time was longer than the processed epoch with the available implementation in MATLAB® (Inc., Natick, Massachusetts, USA, ver. 2019a, interpreted single core implementation, run on a PC with with Intel® Core i7-2630QM, Quad-Core, clock frequency of 2 GHz, 6 GB of RAM and 64 bits operating system). To reduce the computational cost, two methods can be considered: sampling data at 1 kHz (instead of 2 kHz, as before) or shortening the sub-epochs in which the epoch is split (e.g., taking 62.5 ms with 15 ms of overlap). Indeed, the computational cost is about quadratic with respect to the dimension of the processed sub-epoch, as it determines the dimension of the matrix A (including delayed versions of the kernel) which is pseudo-inverted to get the deconvolution. Thus, by reducing the time resolution or the duration of the sub-epochs, the dimension of such a matrix is rapidly reduced and the computational time becomes lower than the duration of the epoch (thus, allowing to process a portion of EMG while sampling new data, without accumulating delays). Figure 7 indicates that the processing time becomes lower than the duration of the processed epoch in both conditions mentioned above and the output of the algorithm is still highly correlated with the simulated CWF. The computational cost could also be reduced by decreasing the number of iterations of the IRLS method (as it depends linearly on the number of iterations).

Thus, in summary, the proposed method applies to single channels of surface EMG and can extract in real time information on global discharges of MUs in the detection volume, opening new potential applications of simple recording systems. However, the method has limitations reflected by the considered interpretation model. Specifically, it was developed and tested assuming that the muscle has parallel fibres and that the detection electrodes are aligned to the fibres. The results are affected by the assumption that all MUAPs have approximately the same shape (possibly rescaled only in amplitude). Thus, complicated conductivity and geometry of the volume conductor (e.g., pinnate muscles with fibres going deep [24]), different directions of propagation of the action potentials [15][23] or misalignment between detection electrodes and muscle fibres (all affecting MUAP shapes) could have a detrimental effect. However, even in the simple simulated conditions, MUAPs shapes already change depending on the relative locations of the MUs with respect to the detection system and on their different CVs. Additional tests, equivalent to those shown in Figure 7, but including a misalignment of 20^o between the muscle fibres and the detection system, indicate that the cross-correlation between the simulated and estimated CWFs decreased in the average by less than 2%. Indeed, in the preliminary tests on experiments (Figure 5), the perfect alignment of the detection electrodes with the fibres is not guaranteed and the output of the algorithm reliably fits the results of an advanced decomposition method exploiting multichannel information. Thus, the method is already tested in conditions in which the modelling hypotheses on which it is based are denied to a certain extent, giving confidence that the information extracted are sta-

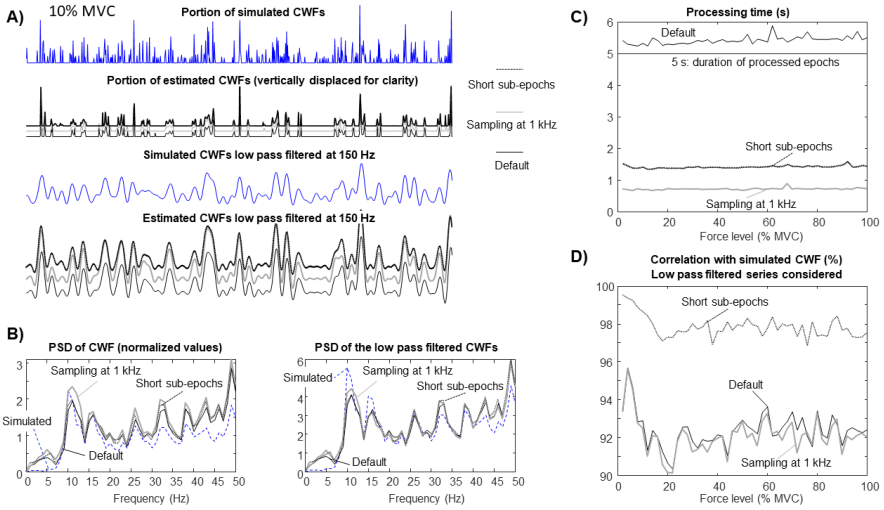

Fig. 7 Investigation of the accuracy and computational costs of different methods: default (i.e., the method considered for the previous figures, considering data sampled at 2 kHz and sub-epochs of 125 ms), short sub-epochs (with duration 62.5 ms) and sampling the EMGs at 1 kHz. A) Cumulative weighted firings (CWF) simulated and estimated by either of the three methods (example of simulated data with force level 10% MVC, no synchronization, fat layer thickness of 7 mm, CoV of ISI 10%). The time series were also low pass filtered with cut-off at 150 Hz (Chebychev type 2 filter), showing that similar low frequency oscillations can be recovered. B) PSD at low frequency (normalized with respect to the mean power) computed from the simulated and estimated CWFs also considered in A (both original and low pass filtered time series are considered; signals of 5 s duration are used). C) Time required by the different methods to process single epochs of EMG of 5 s duration corresponding to different force levels (no synchronization simulated). D) For the same data as in C, correlation between the low pass filtered CWFs either simulated or estimated by the three methods.

ble enough for some applications. Further tests on experimental data are in progress.

5 Conclusions

An innovative method is introduced to estimate the cumulative firings of MUs during a voluntary contraction. It is based on a deconvolution operation applied to surface EMG assuming a kernel which is fit to the data. The method is applied to a single surface EMG channel. Future applications in the study of MU control in different conditions are expected. The possibility of retrieving information on MU firings from a single SD channel makes the method feasible in many conditions in which advanced, high-density recording systems are not available.

References

1. Baker SN, Kilner JM, Pinches EM, Lemon RN (1999) The role of synchrony and oscillations in the motor output. Exp Brain Res. 128(1-2):109-17.
2. Basmajian J, De Luca CJ. Muscles Alive: Their function revealed by electromyography, 5th ed., Williams and Wilkins, Baltimore, 1985.
3. Becker S, von Werder SCFA, Lassek AK, Disselhorst-Klug C (2019) Time-frequency coherence of categorized sEMG data during dynamic contractions of biceps, triceps, and brachioradialis as an approach for spasticity detection. Med Biol Eng Comput. in press.
4. Boyd S, Vandenberghe L, Convex Optimization, Cambridge University Press, 2004.
5. Burrus, C.S. Iterative Reweighted Least Squares. OpenStax CNX. Available online: http://cnx.org/contents/92b90377-2b34-49e4-b26f-7fe572db78a1@12
6. Chen C, Chai G, Guo W, Sheng X, Farina D, Zhu X (2019) Prediction of finger kinematics from discharge timings of motor units: implications for intuitive control of myoelectric prostheses. J Neural Eng. 16(2):026005.
7. Contessa P, Adam A, De Luca CJ (2009) Motor unit control and force fluctuation during fatigue. J Appl Physiol (1985) 107(1):235-43.
8. Contessa P, De Luca CJ (2013) Neural control of muscle force: indications from a simulation model. J Neurophysiol. 109:1548-70.
9. Conway BA, Halliday DM, Farmer SF, Shahani U, Maas P, Weir AI, Rosenberg JR (1995) Synchronization between motor cortex and spinal motoneuronal pool during the performance of a maintained motor task in man. J Physiol. 489 (Pt 3):917-24.
10. Craven D, McGinley B, Kilmartin L, Glavin M, Jones E (2015) Compressed sensing for bioelectric signals: a review, IEEE J. Biomed. Health Inform. 19: 52940.
11. De Luca CJ, Erim Z (1994) Common drive of motor units in regulation of muscle force. Trends Neurosci 17:299305.
12. De Luca CJ, Erim Z (2002) Common drive in motor units of a synergistic muscle pair. J Neurophysiol. 87(4):2200-4.
13. De Luca CJ, Adam A, Wotiz R, Gilmore LD, Nawab SH (2006) Decomposition of surface EMG signals. J Neurophysiol 96: 164657.
14. de Souza LML, Cabral HV, de Oliveira LF, Vieira TM (2018) Motor units in vastus lateralis and in different vastus medialis regions show different firing properties during low-level, isometric knee extension contraction. Hum Mov Sci. 58:307-14.
15. Enck P, Franz H, Davico E, Mastrangelo F, Mesin L, Merletti R (2010) Repeatability of innervation zone identification in the external anal sphincter muscle. Neurourol Urodyn. 29(3): 449-57.
16. Farina D, Merletti R, Enoka RM (2004) The extraction of neural strategies from the surface EMG. J Appl Physiol (1985). 96(4):1486-95. Review.
17. Farina D, Merletti R, Enoka RM (2014) The extraction of neural strategies from the surface EMG: an update. J Appl Physiol (1985). 117(11):1215-30. Review.
18. Herda TJ, Siedlik JA, Trevino MA, Cooper MA, Weir JP (2015) Motor unit control strategies of endurance- versus resistance-trained individuals. Muscle Nerve 52:832843.
19. Holobar A, Zazula D (2007) Multichannel blind source separation using convolution kernel compensation. IEEE Trans. Sig. Proc. 55:448796.
20. Hu X, Suresh AK, Rymer WZ, Suresh NL (2016) Altered motor unit discharge patterns in paretic muscles of stroke survivors assessed using surface electromyography. J Neural Eng. 13(4):046025.
21. Lago PJ, Jones NB (1981) Low-frequency spectral analysis of the e.m.g. Med Biol Eng Comput. 19(6):779-82.
22. Mesin L, Cocito D (2007) A new method for the estimation of motor nerve conduction block. Clinical Neurophysiology. 118(4):730-40.
23. Mesin L, Damiano L, Farina D (2007) Estimation of average muscle fiber conduction velocity from simulated surface EMG in pinnate muscles. J. Neurosci. Methods. 160: 327-34.
24. Mesin L, Merletti R, Vieira TM (2011) Insights gained into the interpretation of surface electromyograms from the gastrocnemius muscles: A simulation study. J. Biomech. 44(6): 1096-103.

25. Mesin L, Dardanello D, Rainoldi A, Boccia G (2016) Motor unit firing rates and synchronisation affect the fractal dimension of simulated surface electromyogram during isometric/isotonic contraction of vastus lateralis muscle. Med. Eng. Phys. 38(12):1530-33.
26. Mesin L (2018) Separation of interference surface electromyogram into propagating and non-propagating components, Biomedical Signal Processing and Control, in press.
27. Mesin L, Non-propagating components of surface electromyogram reflect motor unit firing rates, submitted to IEEE Access 2019.
28. Myers LJ, Lowery M, O'Malley M, Vaughan CL, Heneghan C, St Clair Gibson A, Harley YX, Sreenivasan R (2003) Rectification and non-linear pre-processing of EMG signals for cortico-muscular analysis. J Neurosci Methods. 124(2):157-65.
29. Nawab SH, Chang SS, De Luca CJ (2010) High-yield decomposition of surface EMG signals. Clin Neurophysiol. 121(10):1602-15.
30. Neto OP, Christou EA (2010) Rectification of the EMG signal impairs the identification of oscillatory input to the muscle. J Neurophysiol. 103(2):1093-103.
31. Piitulainen H, Botter A, Bourguignon M, Jousmäki V, Hari R (2015) Spatial variability in cortex-muscle coherence investigated with magnetoencephalography and high-density surface electromyography. J Neurophysiol. 114(5):2843-53.
32. Van Boxtel A, Schomaker LR (1983) Motor unit firing rate during static contraction indicated by the surface EMG power spectrum. IEEE Trans Biomed Eng. 30(9):601-9.
33. Weytjens JL, van Steenberghe D (1984) The effects of motor unit synchronization on the power spectrum of the electromyogram. Biol Cybern. 51(2):71-7.

Luca Mesin graduated in Electronics Engineering in 1999 and received the Ph.D. in Applied Mathematics in 2003 from Politecnico di Torino, Italy. From 2003 to 2008 he was a Fellow of the Laboratory for Neuromuscular System Engineering of the Department of Electronics, Politecnico di Torino. Since 2008, he is Assistant Professor in Biomedical Engineering at the Department of Electronics and Telecommunications and head of the Mathematical Biology and Physiology group (Politecnico di Torino). His main research activities are in the fields of biomedical image/signal processing and mathematical modelling.